UNIVERSITY OF MODENA AND REGGIO EMILIA

PhD Program of Clinical and Experimental Medicine (CEM)

XXXVII Doctorate Cycle
Director of the PhD Program: Prof. Marco Vinceti

Dermoscopy and reflectance confocal microscopy of solitary flat pink lesions: a new combined Score to diagnose amelanotic melanoma

Supervisor: Prof. Caterina Longo

Candidate: Dr. Marco Spadafora

INDEX

PHD YEARS: MY RESEARCH PATH

Over the past 3 years, my academic path allowed me to achieve important skills in non-invasive diagnostic imaging in dermato-oncology, particularly on cutaneous melanoma.

Dermoscopy and reflectance confocal microscopy (RCM) are complementary tools that allows non-invasive diagnosis of skin lesions. Since melanoma is the most aggressive skin tumor, early diagnosis is essential to modify the patient prognosis.

Our group mostly dedicated to early diagnosis of melanoma, identifying dermoscopic features indicating malignancy. The distinctive features of pigmented lesions make them suitable for analysis through dermoscopy, in contrast to amelanotic and hypomelanotic lesions, which typically lack diagnostic clues. Thus, the core subject of my research path was the study of non-pigmented lesions, with a specific focus on amelanotic and hypomelanotic melanoma.[1]

Dermoscopy can be useful to diagnose skin tumors differently from melanoma. Our skin cancer research group with the use of dermoscopy described new clues of rare but insidious skin tumors: trichoepithelioma and trichoblastoma.[2]

Further, the introduction in skin tumor diagnosis of RCM had improved melanoma diagnosis, mostly in non-pigmented or “amelanotic” subtypes difficult to diagnose under dermoscopy. This tool is based on a laser-light source (830 nm wavelength), which specifically targets melanin and cellular organelles, giving a shades-of-grey

digital image. RCM acquired high resolution (0.5 x 0.5 mm2) images at different depths (up to 8x8 mm2 large, up to 250 μm deep). Using RCM on pink lesions, we successfully identify patterns that aid in the prompt diagnosis of amelanotic melanoma.[1]

The use of RCM in dermato-oncology not only allows the study of melanocytic tumors, but also the so-called non-melanoma skin cancers. Our research group recently described the high utility of hand-held RCM for a fast and reliable diagnosis of basal cell carcinoma.[3]

As part of the study of pink lesions under RCM, we have also published a systemic review that showed how dermoscopy and RCM aid in recognizing solitary hypopigmented pink lesion different from melanoma [4].

Moreover, RCM is an effective tool in the aesthetic medicine field. In a recent publication, we showed how RCM is useful in monitoring laser treatment outcomes.[5]

Adjunctively, our research group also reviewed the last 11-year database of Skin Cancer Center in Arcispedale Santa-Maria Nuova di Reggio Emilia, to describe the management of a rare but lethal subtype of melanocytic tumor: mucosal melanoma.[6] We outlined peculiar features according to different mucosal anatomical locations that also influence prognosis.

Further, to understand the biological behavior of squamous cell carcinoma (SCC), an aggressive type of NMSC, we conduct a case-control study on molecular and

histopathological characteristics of metastatic disease, with the recognition of typical molecular signature.[7]

Finally, I also had the opportunity to conduct reasarch in a field different from dermato-oncology. Our group reviewed a new artificial intelligence technology, the natural language processing, that showed promising results when applied to the dermatologic field.[8]

In the final part of this thesis, I reported a complete overview of publications I authored during my PhD course. (See Appendix).

ABSTRACT (EN)

Background: Differential diagnosis of amelanotic/hypomelanotic melanoma among solitary flat pink lesions is challenging, due to limited clinical and dermoscopic clues. Dermoscopy and reflectance confocal microscopy assessments improve diagnostic accuracy, but their combined capacity among solitary flat pink lesions is yet to be defined.

Objectives: To determine (i) whether diagnostic accuracy is improved with combined dermoscopy and reflectance confocal microscopy, (ii) a model to estimate the probability of flat amelanotic/hypomelanotic melanoma among solitary flat pink lesions.

Methods: A retrospective single-center study of solitary flat pink lesions, excised for suspected malignancy between 2011-2022 was performed. Images were independently evaluated by two dermatologists, blinded to histopathological diagnosis. Diagnostic performance was evaluated on the receiver operating characteristic curve and the area under the curve. Predictive features were identified by univariate and multivariate logistic regression analyses. A final predictive nomogram of independent risk factors was calculated by backward likelihood ratio. Hypothesis being tested was formulated before data collection.

Results: A total of 184 patients (87 females, 47.3%) were included; mean age was 57.6 years (19-95). Combined dermoscopy and reflectance confocal microscopy was more sensitive (83%, CI 69.2-92.4 and 91.5%, CI79.6-97.6) than dermoscopy alone (76.6%, CI 62.0-87.7 and 85.1%, CI 71.7-93.8). Predictive features defined the new model, including linear irregular vessels (4.26 folds, CI 1.5-12.1), peripheral pigment network (6.07 folds, CI 1.83-20.15), remnants of pigmentation (4.3 folds, CI 1.27-14.55) at dermoscopy, and atypical honeycomb (9.98 folds, CI 1.91-51.96), disarranged epidermal pattern (15.22 folds, CI 2.18-106.23), dendritic pagetoid cells in the epidermis (3.77 folds, CI 1.25-11.26), hypopigmented pagetoid cells (27.05 folds, CI 1.57-465.5),

and dense and sparse nests (3.68 folds, CI 1.24-10.96) in reflectance confocal microscopy. Diagnostic accuracy of the model was high (AUC 0.91).

Conclusions: Adjunctive reflectance confocal microscopy increases diagnostic sensitivity of flat amelanotic/hypomelanotic melanoma differential diagnosis. The proposed model requires validation.

ABSTRACT (IT)

Background: La diagnosi differenziale del melanoma amelanotico/ipomelanotico tra le lesioni rosa piatte solitarie risulta spesso complessa, a causa dei limitati segni clinici e dermoscopici. L'utilizzo di dermoscopia e microscopia laser confocale migliora l'accuratezza diagnostica, ma la capacità combinata delle due metodiche nello studiuo delle lesioni rosa piatte solitarie deve ancora essere definita.

Obiettivi: Determinare (i) se l'accuratezza diagnostica è superiore utilizzando la dermoscopia combinata alla microscopia laser confocale, (ii) un modello per stimare la probabilità di diagnosticare un melanoma amelanotico/ipomelanotico piatto tra lesioni rosa piatte solitarie della cute.

Metodi: È stato condotto uno studio retrospettivo monocentrico su lesioni rosa piatte solitarie, asportate nel sospetto di malignità tra il 2011-2022. Le immagini sono state valutate in modo indipendente da due dermatologi, in cieco rispetto alla diagnosi istopatologica. La *performance* diagnostica è stata valutata in base alla curva ROC (*receiver operating characteristic*) e all'area sotto la curva. Le caratteristiche predittive sono state identificate mediante analisi di regressione logistica univariata e multivariata. Un nomogramma predittivo dei fattori di rischio indipendenti è stato calcolato mediante il *backward likelihood ratio*. L'ipotesi da testare è stata formulata prima della raccolta dei dati.

Risultati: Sono stati inclusi 184 pazienti (87 femmine, 47,3%); l'età media era di 57,6 anni (19-95). La combinazione di dermoscopia e microscopia laser confocale è risultata più sensibile (83%, CI 69,2-92,4 e 91,5%, CI 79,6-97,6) rispetto alla sola dermoscopia (76,6%, CI 62,0-87,7 e 85,1%, CI 71,7-93,8). Le caratteristiche predittive hanno definito un nuovo modello, comprendente i vasi irregolari lineari (4,26 pieghe, CI 1,5-12,1), il reticolo pigmentato periferico (6,07 pieghe, CI 1,83-20,15), i residui di pigmentazione (4,3 pieghe, CI 1,27-14,55) alla dermoscopia, e l'*honeycomb*

pattern atipico (9,98 pieghe, CI 1,91-51. 96), il pattern epidermico disordinato (15,22 pieghe, CI 2,18-106,23), le cellule pagetoidi dendritiche nell'epidermide (3,77 pieghe, CI 1,25-11,26), le cellule pagetoidi ipopigmentate (27,05 pieghe, CI 1,57-465,5) e i nidi densi e sparsi (3,68 pieghe, CI 1,24-10,96) in microscopia laser confocale. L'accuratezza diagnostica del modello è risultata elevata (AUC 0,91).

Conclusione: L'utilizzo congiunto di microscopia laser confocale e dermoscopia aumenta la sensibilità diagnostica nella diagnosi differenziale del melanoma amelanotico/ ipomelanotico piatto. Il modello proposto richiederà una successiva validazione.

CHAPTER 1

1. GENERAL INTRODUCTION

Solitary pink lesions lack pigmentation which assists in clinical and dermoscopic differential diagnosis[9,10]. Misdiagnosis of amelanotic or hypomelanotic melanoma (AHM) can be fatal, as this subtype of melanoma carries a worse survival than those associated with pigmented melanoma.[10–12]

To improve early AHM detection and differentiation from non-melanocytic pink lesions, non-invasive imaging, such as dermoscopy and reflectance confocal microscopy (RCM), are useful diagnostic technique[9,13,14]. A systematic review and meta-analysis published in 2020 reported the diagnostic accuracy of AHM with dermoscopy or RCM,[15] but the diagnostic accuracy of these combined tools in solitary flat pink lesions is still to be defined.

1.1 EPIDEMIOLOGY AND RISK FACTOR

Melanoma is a malignant tumor originating from melanocytes that in 85% of cases occurs on the skin surface. This type of skin tumor has the highest fatality rate and has seen an increase in prevalence among the white population in the last fifty years. [16,17] The standardized incidence rates in Italy range from 3.9 to 12.5 cases per 100,000 males, with an average of. 6.5) and 3.2 to 13 cases per 100,000 females.[18] The peak incidence is between the fourth and sixth decade of life. Beyond the age of

60, melanoma incidence tends to decrease, except for an increase in the lentigo maligna subtype.[19–21]

The high rate of melanoma in the Caucasian population led to an investigation into genetic and physical characteristics, such as fair skin and sun sensitivity, as potential risk factors for melanoma. People with a large number of melanocytic nevi, especially atypical ones, are identified as a high-risk group. Melanoma appears to be linked to high-intensity UV-ray exposure, on typically unexposed skin areas, and a history of sunburns, particularly during childhood and adolescence. In contrast, lentigo maligna melanoma is determined by cumulative exposure to UV radiation. The biological processes and the specific function of UV rays remain unclear. [19–25]

Among melanoma subtypes, amelanotic melanoma is a rare non-pigmented or hypopigmented subtype of melanoma, comprising only 0.4-27.5% of all melanoma cases. Patients with red hair, type I phototype, freckles, lack of nevi on the back, a sun-sensitive skin are more likely to develop amelanotic melanomas.[26]

Individuals with a history of melanoma have increased risk of developing another primary melanoma, especially within the first two years after the initial diagnosis.[27] Thus, the clinical monitoring of these patients are crucial.

1.2 CLASSIFICATION AND STAGING

Clark introduced a classification in 1969 that differentiated melanoma into three major subtypes by examining clinical and histopathological features, including

superficial spreading melanoma, nodular melanoma, and lentigo maligna.[28] The fourth subtype, acral lentiginous melanoma, was introduced in 1975.[29]

Subsequently, an international group of experts suggested a classification for cutaneous melanoma histotypes, which was later updated, relying on the 1969 Clark's classification.[30] The key difference is seen in the melanoma in situ (noninvasive) and the various types of invasive melanoma. Intraepidermal proliferation of atypical melanocytes characterizes non-invasive melanoma, which includes superficial spreading melanoma, lentigo maligna, and acral lentiginous melanoma. The classification of invasive melanoma includes superficial spreading melanoma, lentigo maligna-melanoma, acral lentiginous melanoma (invasive type), and nodular melanoma. Vertical proliferation is a distinguishing feature of nodular melanoma, in contrast to the other types which exhibit an initial radial-horizontal growth phase confined to the epidermis.

The significance of the primary melanoma's maximum thickness as a prognostic factor was demonstrated by Breslow in 1970.[31] His innovation involved measuring the depth of dermal invasion from the granular layer to the deepest point using a millimeter scale and an ocular micrometer. The reliability and prognostic accuracy of this metric surpassed the previous staging.

The thickness measurement has been validated as the most precise and significant predictor for melanoma staging, leading to its inclusion in the staging protocol. The T stage, in accordance with the American Joint Committee on Cancer (AJCC) staging

guidelines, initially followed Breslow's criteria, but a revision in 2001 led to the classification of melanoma as T0: in situ. T1: ≤ 1 mm; T2: 1-2 mm; T3: 2 to 4 mm; T4> 4 mm[27]. Furthermore, ulceration was included as a separate adverse predictor of outcomes. The progression and natural course of melanoma are influenced by a variety of factors such as age, gender, tumor location, histological type, regression, mitotic activity, and satellitosis.

1.3 *DIAGNOSIS*

Melanoma may develop on healthy skin or on a pre-existing acquired or congenital melanocytic nevus.[32–34] Over the past few years, even though there has been an increase in melanoma diagnoses, mortality rates remained relatively stable because of improved public education, encouraging people to get medical assessments for skin monitoring, and the introduction of new diagnostic techniques and technologies that have improved the precision of melanoma detection. [35–38]

1.3.1 Clinical features

Clinically, cutaneous melanoma is identifiable by irregular shape, a dimension often larger than 6 mm, and a range of colors from pink to brown-black, with areas of uneven pigmentation. It is common for patients to report that the lesion is rapidly growing and presents ulceration, bleeding, and itching. The diagnosis is usually straightforward for lesions that are palpable but may be delayed for lesions in their early stages as they usually present as flat macules or patches.[39] Self-assessment is

crucial for the early detection of melanoma, especially for individuals in risk groups. Patients who conduct periodic self-checks of their skin surface demonstrate melanomas with a markedly decreased Breslow thickness when compared to those who do not.[40]

1.3.2 Dermoscopy

Dermoscopy, also known as dermatoscopy or epiluminescence microscopy, was introduced in the late 1980s as a valuable method to study pigmented lesions, enhancing diagnostic precision over clinical inspection.[41,42] It is a non-invasive diagnostic technique that enables the examination of morphological features beneath the skin's surface, which are typically unseen by the naked eye. Through this method, melanoma can be distinguished from other melanocytic and non-melanocytic skin lesions. The recognition of specific pigmented and non-pigmented structures aids dermatologists in assessing equivocal lesions and detecting lesions most likely to be malignant. Studies have demonstrated a 60-90% enhancement in diagnostic precision when utilizing this tool over conventional clinical assessment methods. [43–45] The expertise of dermatologists plays a crucial role in the superior performance of this tool compared to clinical observation, especially in detecting early-stage melanomas.[46,47]

As amelanotic-hypopigmented melanoma lacks pigmentation, its appearances vary and can mimic many benign and malignant conditions, thus presenting a diagnostic challenge.[39,48]

1.3.3 Reflectance confocal microscopy

While dermoscopy improved diagnostic precision in the diagnosis of pigmented skin lesions, the detection of featureless melanomas, such as AHM, continued to pose a challenge. This inaccuracy required the excise of four-fold benign lesions for every melanoma, to maintain a high diagnostic sensitivity even by expert observers. [44]

In vivo confocal laser microscopy allows for a more precise examination of skin cancers, leading to early detection without causing any discomfort to the patient. It provides a fast noninvasive scan of the epidermis and superficial dermis, with a resolution close to that of histological samples. [49,50]

In dermato-oncology, it can aid in the precise diagnosis of epithelial tumors such as basal cell carcinoma, Bowen's disease, and squamous cell carcinoma, distinguishing them from benign and malignant melanocytic lesions, reducing unnecessary excisions.[51–53]

1.3.3.1 Technical aspects

The functioning principle of the confocal laser is based on a point light source; the light is emitted by a 830 nm wavelength laser and is focused through a pinhole diaphragm to one point on the object. The reflected laser light is separated by a beam splitter from the incident laser beam path and is deflected through a second confocal diaphragm to reach a photosensitive detector. Because of the confocal design, light originating from outside the focal plane is highly suppressed, and only the object

layer located at the focal plane contributes to the image. To build a 2D image of a thin layer of the skin, perpendicular to the optical axis of the device (then, horizontal with respect to the skin surface), the laser beam has to scan the sample point by point; this is achieved by introducing oscillating mirrors into the beam path. By optical movement on the focal plane, an image can be acquired from a deeper layer of the examined object, thus enabling a data cube to be built up in a successive series. The light diffusion and reflectance vary according to the different refraction indices of the encountered particles compared to the surrounding skin. [49,50,54]

1.3.3.2 Acquisition methods

The commercially available Confocal Microscope (Vivascope 1500, Lucid Inc, Rochester, New York) consists of a scanning unit mounted on an articulating arm for positioning on the patient. A metal ring fixed by an adhesive window is applied onto the skin. The microscope is then coupled to the metal ring by a magnet on the arm of the microscope. Thereby a stable contact between the skin and the objective lens is created. A gel or an oily solution with a refractive index close to that of water (i.e. 1.33) is placed between the objective lens and the tissue, and within the metal ring prior to contact.

With a 30X lens, the field of view in the tissue is 0.5 x 0.5 mm, corresponding to 1000 x 1000 pixels. However, larger fields of view are achievable by “stitching” together, via computer software, sequentially acquired adjacent images to create and display a mosaic. The current version of this software allows up to 16 x 16 images to

be “stitched” together, thereby creating and displaying a ”block” images). Moreover, it is possible to acquire succeeding images in the same tissue section, reproducing in this way dynamic events, up to recording short videoclips, or deeper and deeper horizontal sections of the same detailed area (“stack” modality).

According to the opening of the objective lens and of the diaphragm, different wavelengths are achieved, to produce variations in the resolution of the produced images: the best compromise between a good penetration depth and a good image resolution was reached using a 830 nm wavelength, with a low laser power (30 mW), not inducing a perceivable local heating.

The use of a near-infrared wavelength of 830 nm permits imaging to depths of up to 200-250 μm in normal skin, allowing the visualization of the epidermis and superficial dermis, with a lateral resolution of 0.5-1 μm, and an axial resolution of 4-5 μm.

Acquired images show chromatic variations on the grey scale (256 colors), therefore more reflective cells and particles are white colored, while hypo-reflective ones are dark gray to black.

The main limitation of confocal microscopy is the depth of penetration of the light source, hampering the evaluation of structures located beyond 200-300 μm deep, such as deep neoplasms (such as cutaneous lymphomas or adnexal tumors) or very hyperkeratotic lesions (such as hyperkeratotic actinic keratosis)[55] Further, image

interpretation and evaluation of peculiar cell type require specifically trained clinicians.[56]

Despite the limitations, this device serves as a secondary assessment for selected equivocal lesions on clinical and dermoscopic examinations, providing cyto-architectural details that closely resemble histological ones. It plays a crucial role in reaching the correct diagnosis, especially in cases where dermoscopic features are challenging to interpret.

The combination of confocal microscopy and dermoscopy offers a substantial advancement in accurately diagnosing skin cancer, particularly melanoma, and helps in avoiding unnecessary excisions or missed diagnosis. [14,57–60]

CHAPTER 2

2. OBJECTIVES

The primary aim of this study is to compare the diagnostic accuracy of dermoscopy alone to that of combined dermoscopy and RCM in detecting flat AHM (fAHM) in a subset of solitary flat pink lesions. Our secondary aim is to propose a combined dermoscopy and RCM model to predict the probability of fAHM in clinical practice.

CHAPTER 3

3. MATERIALS AND METHODS

3.1 Patient selection

A retrospective, single-center, observational study reviewed consecutive solitary, pink-colored macules or patches of the skin assessed with clinical, dermoscopy, RCM, and histopathological evaluations between January 2011 to December 2022 for study inclusion (Fig. 1). All patients were treated at the Skin Cancer Center of the Arcispedale Santa Maria Nuova in Reggio Emilia, Italy.

Predefined criteria specified the inclusion of dermoscopy images with pigmentation areas in <25% [9] and the exclusion of lesions with histopathologically confirmed inflammatory and infectious diseases. Lesions were retrospectively identified from a center database by one trained dermatologist (M.S.).

Standardized polarized dermoscopic images were obtained with DermLite Photo (3Gen, San Juan Capistrano, CA, USA) mounted on a Canon G16 camera. RCM imaging was performed with the VivaScope 1500 (Mavig GmbH, Munich, Germany).

Lesion image sets were blinded to histopathological diagnoses. Clinical and dermoscopy images were united for initial dermoscopy assessment, and then a complete set (clinical, dermoscopy and RCM) was provided in a second time frame for combined dermoscopy and RCM evaluations. Image sets were casually presented. All images were evaluated by two dermatologists with at least 5 years of expertise in dermoscopy and RCM (AM and NL). Images were analyzed for the presence of selected dermoscopy and RCM criteria from literature, Table 2.[13,14,58,61–74] Evaluators were asked to formulate a diagnosis based on clinical and dermoscopic images first, then on dermoscopy and RCM images of the same lesion. Clinical data (age at diagnosis, gender, and site of the lesion) were retrieved from the Hospital Clinical Database.

A subgroup analysis of the misdiagnosis assigned to false negatives following combined dermoscopy and RCM was performed.

3.2 Statistical analysis

Statistical analysis was performed using STATA® software version 17 (StataCorp. 2021. Stata Statistical Software: Release 17. College Station, TX: StataCorp LLC.)

and MedCalc Statistical Software version 14.8.1 (MedCalc Software bvba, Ostend, Belgium; http://www.medcalc.org; 2014). Continuous variables were presented as the number of patients (No), mean, standard deviation (SD), minimum (min), and maximum (max) and compared using Unpaired Student's t-test. Categorical variables were presented as frequency (No, percentage [%]) and compared using Pearson's chi-squared test. Cohen's kappa (κ) statistic evaluated the agreement between dermoscopic or RCM diagnosis and histopathological diagnosis (binary variable); less than chance ($\kappa < 0$), slight ($\kappa = 0.01$ to 0.20), fair ($\kappa = 0.21$ to 0.40), moderate ($\kappa = 0.41$ to 0.60), substantial ($\kappa = 0.61$ to 0.80), and almost perfect ($\kappa = 0.81$ to 0.99) agreement. Diagnostic performance is evaluated on the receiver operating characteristic (ROC) curve and the area under the curve (AUC). Univariate and multivariate logistic regression models were carried out using a stepwise selection method to identify prognostic factors between groups. “Goodness of fit” with the Hosmer and Lemeshow test evaluated the selection model. Data from logistic regression analyses are expressed as odds ratio (OR) and 95% confidence interval (CI). The backward likelihood ratio method was employed to create a final multivariate model and develop a nomogram of independent risk factors. Predictability of the nomogram was assessed by AUC in ROC analysis. For all analyses, a $P<.05$ was considered statistically significant.

CHAPTER 4

4. RESULTS

4.1 Population

The study included 184 solitary flat pink lesions in 184 patients (87 females, 47.3%), demographic and lesion anatomical data are outlined in Table 2. Average age at diagnosis was significantly different among fAHM and non-fAHM patients (55.8 ±13.8 in non-fAHM and 62.6 ±14.2 in fAHM, P=.004). fAHM diagnoses were made in 47 lesions (25.5%). Other diagnoses included 62 basal cell carcinomas (BCCs), 22 dermatofibromas (DFs), 7 lichen planus-like keratosis (LPLK), 5 actinic keratosis (AKs), 5 Bowen diseases (BDs), 5 seborrheic keratosis (SKs) and 31 naevi. (Table 3)

4.2 Diagnostic accuracy of dermoscopy and RCM

A moderate agreement was observed between the 2 independent evaluators at dermoscopy alone and combined dermoscopy and RCM (κ=56.5 and 57.4). A sub-analysis of false negative lesions following combined RCM and dermoscopy assessment revealed that all false negatives were misdiagnosed as BCCs, with the exception of a dermatofibroma (n=1/12) (Table 3). The association of RCM with dermoscopy assessment increased sensitivity with variable specificity values, compared to dermoscopy alone (Table 4)

The overall diagnostic accuracy for fAHM measured by AUC was 0.82 in dermoscopy for both evaluators, 0.81 and 0.86 in RCM respectively, see Table 4.

Subgroup analyses of false negatives following combined dermoscopy and RCM identified the absence of independent diagnostic features typical of AHM or BCC, with the presence of shared features only. Specifically, features included atypical junctional cells with disarrangement and hypo-reflective structures surrounded by dark areas.

4.3 Univariate, multivariate analysis and predictive nomogram of fAHM diagnosis in a group of solitary flat pink lesions

Univariate analysis vessels-related dermoscopic criteria associated with the diagnosis of fAHM included dotted vessels (OR 4.22, CI 1.94-9.16, P<.001), linear irregular vessels (OR 6.05, CI 2.93-12.45, P<.001) and polymorphous vessels (OR 5.92, CI 2.61-13.44, P<.001); vascular features which were negative predictors of fAHM were arborizing vessels (OR 0.23, CI 0.09-0.56, P=.001) and fine telangiectasia (OR 0.10, CI 0.01-0.82, P=.03). Pigment-related dermoscopic parameters predictive of fAHM were peripheral pigment network (OR 2.52, CI 1.22-5.21, P=.01), negative pigment network (OR 7.13, CI 2.29-22.17, P=.001), and remnants of pigmentation (OR 4.92, CI 2.14-11.30, P<.001). White-pink background was a negative predictor of fAHM (OR 0.16, CI 0.05-0.47, P=.001). (Table 5)

On RCM evaluations, irregular honeycomb (OR 13.6, CI 3.11-59.5, P=.001) and disarranged epidermal patterns (OR 4.22, CI 8.92-220.6, P<.001) were associated

with the diagnosis of fAHM. Furthermore, the presence of roundish (OR 12.18, CI 5.55-26.73, P<.001), dendritic (OR 8.69, CI 4.13-18.28, P<.001), and hyporeflective pagetoid cells (OR 16.07, CI 1.82-141.43, P=.012), sheet of cells (OR 3.78, CI 1.28-11.08, P=.015), atypical junctional cells (OR 10.65, CI 4.95-22.90, P<.001), and dense and sparse nest (OR=10.32, CI 4.82-22.09, P<.001) led to a significantly increased risk of diagnosing fAHM on RCM. On the other hand, the univariate model showed that tumor islands (OR 0.20, CI 0.08-0.49, P<.001), clefting (OR 4.22, CI 0.07-0.55, P=.002), and thickened collagen bundles (OR 0.17, CI 0.06-0.43, P<.001) were negative predictors of fAHM.

The Nomogram (Fig. 2a) includes predictive variables identified with multivariate model (Table 5) and was used to create the fAHM Index. The fAHM Index includes weighted score criteria: 3 dermoscopic parameters (linear irregular vessels, peripheral pigment network, and remnants of pigmentation) and 4 RCM parameters (atypical honeycomb and disarranged epidermal pattern, dendritic pagetoid cells in the epidermis, hypopigmented pagetoid cells and dense and sparse nests). The predictive accuracy was classified as high (AUC= 0.91) (Fig. 2b). Criteria are presented in a worksheet (Table 6), to assist clinicians in calculating the probability of fAHM diagnosis. The fAHM Index was applied to selected solitary pink lesions (Fig. 3)

CHAPTER 5

5. GENERAL DISCUSSION AND CONCLUSION

5.1 *Discussion*

In our study, adjunctive use of RCM in the assessment of solitary flat pink lesions proved to increase melanoma diagnostic sensitivity compared to dermoscopy alone. The fAHM Index, with the integration of independent dermoscopy and RCM diagnostic features, assists clinicians in assessing the probability of fAHM differential diagnosis among solitary flat pink lesions.

Our study confirms previous observations of dermoscopy[9,63,75] and RCM[14,58,61,76] criteria associated with AHM, with both univariate and multivariate analyses. In amelanotic melanoma, it has been noted that linear irregular vessels may be the only suspicious dermoscopic diagnostic clue[9,63], whereas, in hypopigmented melanoma, the adjunctive predictive clues of peripheral pigment network and remnants of pigmentation can enhance the probability of fAHM diagnosis. Linear irregular vessels were found in our study to increase the chances of a fAHM diagnosis by 4.5 times. Interestingly, peripheral pigment network, usually associated with DF diagnoses, was an independent clue for fAHM, increasing the likelihood of diagnosis by more than 5 times[64]. When associated with fAHM, peripheral pigment network may appear as fine, at the periphery of the lesion, usually interrupted and incomplete in the whole perimeter. Peripheral pigment network combined with other melanoma

clues, has previously been noted as indicative of melanoma diagnosis in flat lesions[77]. Remnants of pigmentation in fAHM usually present as faded pigment with no discernible structure, with or without peppering, at the periphery or discretely diffused within the lesion, and was found in our study to increase the chance of a fAHM diagnosis by more than 4 times. The authors suggest that the observation of remnants of pigmentation is usually subtle (faded) and requires an in-depth study of dermoscopy images.

Under RCM, the level of epidermal pattern disruption in the suprabasal layer correlates with an increasing risk of fAHM diagnoses. This observation has been previously reported in amelanotic melanoma series[59]. We described a spectrum ranging from regular honeycomb (low risk), atypical honeycomb (medium-high risk) to disarranged epidermal pattern (high risk). Observing dendritic pagetoid cells in a solitary pink lesion increases the probability of diagnosing fAHM 4 fold[59,78]. Hyporeflective pagetoid cells increase the chance of fAHM diagnosis by 10 times. Hyporeflective cells have already been described[14,59] as independently specific for AHM and in the differential diagnoses of melanomas from other non-pigmented tumors. Finally, dense and sparse nests increase the likelihood of a fAHM diagnosis by four times, data already confirmed in literature[58,78]. The fAHM Index predicts the probability of fAHM diagnosis according to the independent dermoscopy and RCM criteria identified in our study of solitary, exclusively flat, pink lesions.

Subgroup analysis of misdiagnosed lesions following combined dermoscopy and RCM evaluations revealed BCC diagnoses in all false negative cases. It has already been reported that BCC can exhibit shared RCM criteria with atypical melanocytic lesions, particularly cell atypia[59]. False negatives observations confirm previous assumptions that hyporeflective/non-reflective areas and disarrangement render differential diagnoses of pink melanoma from BCC complex[59].

Our study reports higher sensitivity rates with combined dermoscopy and RCM evaluations compared to dermoscopy alone (76.6-85.1% vs 83.0 – 91.5%). fAHM diagnostic dermoscopy features are considered more difficult to observe, and this may explain the comparable lower rates of sensitivity observed with dermoscopy [9,77,79]. In a subtype of melanoma considered "difficult to diagnose" with worse prognoses than pigmented counterparts, a higher sensitivity of diagnostic techniques (reduced number of false negatives) should be paramount. A recent review and metanalysis by Lan et al., including 1,111 lesions from 7 studies, reported pooled AHM sensitivity rates of dermoscopy of 61% (95% CI 0.37–0.81) and for RCM alone (537 lesions from 3 studies) of 67% (95% CI 0.51–0.81).[15] Compared to these estimates, we suggest that the combined approach may be likely to increase diagnostic sensitivity by 10-15% points. A recently published randomized control trial [80] shows that adjunctive use of RCM for suspect lesions assures the removal of aggressive melanomas at baseline in a real-life, clinical decision-making application for referral centers with RCM.

Models to assist in the detection of AHM with dermoscopy have been proposed. From the first description of vessel morphology among early amelanotic melanoma[74], progress in diagnostic sensitivity and specificity of dermoscopy alone has been made. Menzies et al.[9] proposed 2 dermoscopic models for the detection of malignancies among "lesions lacking significant pigment." Both models are based on negative and positive criteria, with sensitivity and specificity levels ranging from 77 - 97% and 41-79%, respectively. Subsequently, Russo et al. [79] showed that through the application of a 'prevalent criterion' approach, i.e., the most representative dermoscopic feature, sensitivity and specificity could be raised to 93.2% and 83.1%.

Studies of the efficacy of RCM in AHM differential diagnosis available in literature are difficult to compare based on heterogeneous lesion inclusion criteria. RCM in AHM was first studied by Guitera et al. in a subgroup of light-colored melanocytic lesions (31 nevi and 13 melanomas)[60]. A subsequent study by the same research team included amelanotic and light-colored flat or palpable lesions (macules, papules, and nodules). [59] Witkowski et al.[67] included equivocal pink lesions with suspected BCC diagnoses only. Braga et al. [68] describeb AHM cases without testing accuracy of RCM criteria. Cinotti et al. [81] and Pizzichetta et al. [78] more recently reported dermoscopy and RCM features of facial amelanotic lentigo maligna. However, predictive models to support differential diagnosis with RCM and dermoscopy have not been reported in literature. We propose a positive scoring system, based on independent dermoscopy and RCM features reported in this study for rapid and complete assessment of equivocal solitary flat pink lesions.

5.2 *Limitations*

This study has inherent limitations due to the retrospective nature of the study design. However, all efforts were made to blind recovered images to histopathological diagnoses for prospectively unbiased evaluations. The heterogeneous sample of equivocal solitary flat pink lesions only rendered the sample size relatively restricted. However, the inclusion criteria of this heterogeneous group were designed to mimic lesions observed in clinical practice settings and to assist in early melanoma identification. The proposed fAHM Index has not been validated and requires assessment on a separate data set.

5.3 *Conclusion*

Adjunctive RCM improves fAHM diagnostic accuracy among equivocal solitary flat pink lesions, with a higher sensitivity than dermoscopy alone. The proposed fAHM Index assists in improving diagnostic precision of solitary flat pink lesions.

CHAPTER 6

6. REFERENCES

1. Spadafora M, Megna A, Lippolis N, *et al.* Dermoscopy and reflectance confocal microscopy of solitary flat pink lesions: A new combined score to diagnose amelanotic melanoma. *J Eur Acad Dermatol Venereol* 2024.

2. Dermoscopic features of trichoepithelioma: A multicentre observational case-control study conducted by the International Dermoscopy Society - PubMed. https://pubmed.ncbi.nlm.nih.gov/37326166/. Accessed 20 Oct 2024.

3. Longo C, Guida S, Mirra M, *et al.* Dermoscopy and reflectance confocal microscopy for basal cell carcinoma diagnosis and diagnosis prediction score: a prospective and multicenter study on 1005 lesions. *J Am Acad Dermatol* 2024;:S0190-9622(24)00135-X.

4. Ambrosio L, Pogorzelska-Antkowiak A, Retrosi C, *et al.* Reflectance Confocal Microscopy and Dermoscopy for the Diagnosis of Solitary Hypopigmented Pink Lesions: A Narrative Review. *Cancers* 2024;**16**:2972.

5. Guida S, Longo C, Amato S, *et al.* Laser Treatment Monitoring with Reflectance Confocal Microscopy. *Medicina (Kaunas)* 2023;**59**:1039.

6. Spadafora M, Santandrea G, Lai M, *et al.* Clinical Review of Mucosal Melanoma: The 11-Year Experience of a Referral Center. *Dermatol Pract Concept* 2023;**13**:e2023057.

7. Paganelli A, Zaffonato M, Donati B, *et al.* Molecular and Histopathological

Characterization of Metastatic Cutaneous Squamous Cell Carcinomas: A Case-Control Study. *Cancers (Basel)* 2024;**16**:2233.

8. Paganelli A, Spadafora M, Navarrete-Dechent C, Guida S, Pellacani G, Longo C. Natural language processing in dermatology: A systematic literature review and state of the art. *J Eur Acad Dermatol Venereol* 2024.

9. Menzies SW, Kreusch J, Byth K, *et al.* Dermoscopic evaluation of amelanotic and hypomelanotic melanoma. *Arch Dermatol* 2008;**144**:1120–7.

10. Strazzulla LC, Li X, Zhu K, Okhovat J-P, Lee SJ, Kim CC. Clinicopathologic, misdiagnosis, and survival differences between clinically amelanotic melanomas and pigmented melanomas. *J Am Acad Dermatol* 2019;**80**:1292–8.

11. Cheung WL, Patel RR, Leonard A, Firoz B, Meehan SA. Amelanotic melanoma: a detailed morphologic analysis with clinicopathologic correlation of 75 cases. *J Cutan Pathol* 2012;**39**:33–9.

12. Shen S, Wolfe R, McLean CA, Haskett M, Kelly JW. Characteristics and associations of high-mitotic-rate melanoma. *JAMA Dermatol* 2014;**150**:1048–55.

13. Gill M, González S. Enlightening the Pink: Use of Confocal Microscopy in Pink Lesions. *Dermatol Clin* 2016;**34**:443–58.

14. Losi A, Longo C, Cesinaro AM, *et al.* Hyporeflective pagetoid cells: a new clue for amelanotic melanoma diagnosis by reflectance confocal microscopy. *Br J Dermatol* 2014;**171**:48–54.

15. Lan J, Wen J, Cao S, *et al.* The diagnostic accuracy of dermoscopy and reflectance confocal microscopy for amelanotic/hypomelanotic melanoma: a

systematic review and meta-analysis. *Br J Dermatol* 2020;**183**:210–9.

16. Coleman MP, Estève J, Damiecki P, Arslan A, Renard H. Trends in cancer incidence and mortality. *IARC Sci Publ* 1993;:1–806.

17. E de V, Jw C. Cutaneous malignant melanoma in Europe. *European journal of cancer (Oxford, England : 1990)* 2004;**40**doi:10.1016/j.ejca.2004.06.003.

18. AIRTUM Working Group 2018 | Associazione Italiana Registri Tumori. https://www.registri-tumori.it/cms/pagine/airtum-working-group-2018. Accessed 7 Oct 2024.

19. Markovic SN, Erickson LA, Rao RD, *et al.* Malignant melanoma in the 21st century, part 1: epidemiology, risk factors, screening, prevention, and diagnosis. *Mayo Clin Proc* 2007;**82**:364–80.

20. Rastrelli M, Tropea S, Rossi CR, Alaibac M. Melanoma: epidemiology, risk factors, pathogenesis, diagnosis and classification. *In Vivo* 2014;**28**:1005–11.

21. Whiteman DC, Whiteman CA, Green AC. Childhood sun exposure as a risk factor for melanoma: a systematic review of epidemiologic studies. *Cancer Causes Control* 2001;**12**:69–82.

22. Kuphal S, Bosserhoff A. Recent progress in understanding the pathology of malignant melanoma. *J Pathol* 2009;**219**:400–9.

23. Jl B. Site-specific risk of cutaneous malignant melanoma and pattern of sun exposure in New Zealand. *International journal of cancer* 2000;**85**doi:10.1002/(sici)1097-0215(20000301)85:5<627::aid-ijc5>3.0.co;2-y.

24. Wachsmuth RC, Turner F, Barrett JH, *et al.* The effect of sun exposure in

determining nevus density in UK adolescent twins. *J Invest Dermatol* 2005;**124**:56–62.

25. Gandini S, Sera F, Cattaruzza MS, *et al.* Meta-analysis of risk factors for cutaneous melanoma: III. Family history, actinic damage and phenotypic factors. *Eur J Cancer* 2005;**41**:2040–59.

26. Gong H-Z, Zheng H-Y, Li J. Amelanotic melanoma. *Melanoma Res* 2019;**29**:221–30.

27. Balch CM, Soong SJ, Gershenwald JE, *et al.* Prognostic factors analysis of 17,600 melanoma patients: validation of the American Joint Committee on Cancer melanoma staging system. *J Clin Oncol* 2001;**19**:3622–34.

28. Clark WH, From L, Bernardino EA, Mihm MC. The histogenesis and biologic behavior of primary human malignant melanomas of the skin. *Cancer Res* 1969;**29**:705–27.

29. Reed RJ, Ichinose H, Clark WH, Mihm MC. Common and uncommon melanocytic nevi and borderline melanomas. *Semin Oncol* 1975;**2**:119–47.

30. McGovern VJ, Cochran AJ, Van der Esch EP, Little JH, MacLennan R. The classification of malignant melanoma, its histological reporting and registration: a revision of the 1972 Sydney classification. *Pathology* 1986;**18**:12–21.

31. A B. Thickness, cross-sectional areas and depth of invasion in the prognosis of cutaneous melanoma. *Annals of surgery* 1970;**172**doi:10.1097/00000658-197011000-00017.

32. Krengel S, Hauschild A, Schäfer T. Melanoma risk in congenital melanocytic

naevi: a systematic review. *Br J Dermatol* 2006;**155**:1–8.

33. Caccavale S, Calabrese G, Mattiello E, *et al.* Cutaneous Melanoma Arising in Congenital Melanocytic Nevus: A Retrospective Observational Study. *Dermatology* 2021;**237**:473–8.

34. Kinsler VA, O'Hare P, Bulstrode N, *et al.* Melanoma in congenital melanocytic naevi. *Br J Dermatol* 2017;**176**:1131–43.

35. Cayuela A, Rodríguez-Domínguez S, Lapetra-Peralta J, Conejo-Mir JS. Has mortality from malignant melanoma stopped rising in Spain? Analysis of trends between 1975 and 2001. *Br J Dermatol* 2005;**152**:997–1000.

36. Weinstock MA. Cutaneous melanoma: public health approach to early detection. *Dermatol Ther* 2006;**19**:26–31.

37. Geller AC, Zhang Z, Sober AJ, *et al.* The first 15 years of the American Academy of Dermatology skin cancer screening programs: 1985-1999. *J Am Acad Dermatol* 2003;**48**:34–41.

38. Koh HK, Geller AC, Miller DR, Lew RA. The early detection of and screening for melanoma. International status. *Cancer* 1995;**75** 2 Suppl:674–83.

39. Cabrera R, Recule F. Unusual Clinical Presentations of Malignant Melanoma: A Review of Clinical and Histologic Features with Special Emphasis on Dermatoscopic Findings. *Am J Clin Dermatol* 2018;**19** Suppl 1:15–23.

40. Pollitt RA, Geller AC, Brooks DR, Johnson TM, Park ER, Swetter SM. Efficacy of skin self-examination practices for early melanoma detection. *Cancer Epidemiol Biomarkers Prev* 2009;**18**:3018–23.

41. Pehamberger H, Steiner A, Wolff K. In vivo epiluminescence microscopy of pigmented skin lesions. I. Pattern analysis of pigmented skin lesions. *J Am Acad Dermatol* 1987;**17**:571–83.

42. Soyer HP, Smolle J, Leitinger G, Rieger E, Kerl H. Diagnostic reliability of dermoscopic criteria for detecting malignant melanoma. *Dermatology* 1995;**190**:25–30.

43. Bafounta ML, Beauchet A, Aegerter P, Saiag P. Is dermoscopy (epiluminescence microscopy) useful for the diagnosis of melanoma? Results of a meta-analysis using techniques adapted to the evaluation of diagnostic tests. *Arch Dermatol* 2001;**137**:1343–50.

44. P C, V DG, E C, *et al.* Improvement of malignant/benign ratio in excised melanocytic lesions in the "dermoscopy era": a retrospective study 1997-2001. *The British journal of dermatology* 2004;**150**doi:10.1111/j.0007-0963.2004.05860.x.

45. Tromme I, Sacré L, Hammouch F, *et al.* Availability of digital dermoscopy in daily practice dramatically reduces the number of excised melanocytic lesions: results from an observational study. *Br J Dermatol* 2012;**167**:778–86.

46. Argenziano G, Soyer HP. Dermoscopy of pigmented skin lesions--a valuable tool for early diagnosis of melanoma. *Lancet Oncol* 2001;**2**:443–9.

47. Me V, P M, Pe H, Sw M. Dermoscopy compared with naked eye examination for the diagnosis of primary melanoma: a meta-analysis of studies performed in a clinical setting. *The British journal of dermatology* 2008;**159**doi:10.1111/j.1365-2133.2008.08713.x.

48. Stojkovic-Filipovic J, Kittler H. Dermatoscopy of amelanotic and hypomelanotic melanoma. *J Dtsch Dermatol Ges* 2014;**12**:467–72.

49. Rajadhyaksha M, Grossman M, Esterowitz D, Webb RH, Anderson RR. In vivo confocal scanning laser microscopy of human skin: melanin provides strong contrast. *J Invest Dermatol* 1995;**104**:946–52.

50. Rajadhyaksha M, González S, Zavislan JM, Anderson RR, Webb RH. In vivo confocal scanning laser microscopy of human skin II: advances in instrumentation and comparison with histology. *J Invest Dermatol* 1999;**113**:293–303.

51. Peris K, Fargnoli MC, Kaufmann R, *et al.* European consensus-based interdisciplinary guideline for diagnosis and treatment of basal cell carcinoma-update 2023. *Eur J Cancer* 2023;**192**:113254.

52. Stratigos AJ, Garbe C, Dessinioti C, *et al.* European interdisciplinary guideline on invasive squamous cell carcinoma of the skin: Part 1. epidemiology, diagnostics and prevention. *Eur J Cancer* 2020;**128**:60–82.

53. Garbe C, Amaral T, Peris K, *et al.* European consensus-based interdisciplinary guideline for melanoma. Part 1: Diagnostics: Update 2022. *Eur J Cancer* 2022;**170**:236–55.

54. Pellacani G, Seidenari S. In vivo reflectance mode confocal laser microscopy of melanocytic skin lesions. In: Handbook of non-invasive methods and the skin, Eds. J Serup, GBE Jemec, G Grove; CRC Press, Boca Raton, Florida, Usa, 2005 (2nd ed). .

55. Busam KJ, Marghoob AA, Halpern A. Melanoma diagnosis by confocal microscopy: promise and pitfalls. *J Invest Dermatol* 2005;**125**:vii.

56. Hashemi P, Pulitzer MP, Scope A, Kovalyshyn I, Halpern AC, Marghoob AA. Langerhans cells and melanocytes share similar morphologic features under in vivo reflectance confocal microscopy: a challenge for melanoma diagnosis. *J Am Acad Dermatol* 2012;**66**:452–62.

57. Carrera C, Palou J, Malvehy J, *et al.* Early stages of melanoma on the limbs of high-risk patients: clinical, dermoscopic, reflectance confocal microscopy and histopathological characterization for improved recognition. *Acta Derm Venereol* 2011;**91**:137–46.

58. Pellacani G, Guitera P, Longo C, Avramidis M, Seidenari S, Menzies S. The impact of in vivo reflectance confocal microscopy for the diagnostic accuracy of melanoma and equivocal melanocytic lesions. *J Invest Dermatol* 2007;**127**:2759–65.

59. Guitera P, Menzies SW, Argenziano G, *et al.* Dermoscopy and in vivo confocal microscopy are complementary techniques for diagnosis of difficult amelanotic and light-coloured skin lesions. *Br J Dermatol* 2016;**175**:1311–9.

60. Guitera P, Pellacani G, Longo C, Seidenari S, Avramidis M, Menzies SW. In vivo reflectance confocal microscopy enhances secondary evaluation of melanocytic lesions. *J Invest Dermatol* 2009;**129**:131–8.

61. Longo C, Moscarella E, Argenziano G, *et al.* Reflectance confocal microscopy in the diagnosis of solitary pink skin tumours: review of diagnostic clues. *Br J Dermatol* 2015;**173**:31–41.

62. Zalaudek I, Giacomel J, Argenziano G, *et al.* Dermoscopy of facial nonpigmented actinic keratosis. *Br J Dermatol* 2006;**155**:951–6.

63. Giacomel J, Zalaudek I. Pink lesions. *Dermatol Clin* 2013;**31**:649–78, ix.

64. Agero ALC, Taliercio S, Dusza SW, Salaro C, Chu P, Marghoob AA. Conventional and polarized dermoscopy features of dermatofibroma. *Arch Dermatol* 2006;**142**:1431–7.

65. Fink C, Haenssle HA. Non-invasive tools for the diagnosis of cutaneous melanoma. *Skin Res Technol* 2017;**23**:261–71.

66. Navarrete-Dechent C, Liopyris K, Monnier J, *et al.* Reflectance confocal microscopy terminology glossary for melanocytic skin lesions: A systematic review. *J Am Acad Dermatol* 2021;**84**:102–19.

67. Witkowski AM, Łudzik J, DeCarvalho N, *et al.* Non-invasive diagnosis of pink basal cell carcinoma: how much can we rely on dermoscopy and reflectance confocal microscopy? *Skin Res Technol* 2016;**22**:230–7.

68. Braga JCT, Scope A, Klaz I, *et al.* The significance of reflectance confocal microscopy in the assessment of solitary pink skin lesions. *J Am Acad Dermatol* 2009;**61**:230–41.

69. Ferrari F, Bassoli S, Pellacani G, Argenziano G, Cesinaro AM, Longo C. Similar but Different: How Reflectance Confocal Microscopy May Help in the Diagnosis of Pink Lesions. *Dermatology* 2017;**233**:212–6.

70. Haspeslagh M, Noë M, De Wispelaere I, *et al.* Rosettes and other white shiny structures in polarized dermoscopy: histological correlate and optical explanation. *J Eur Acad Dermatol Venereol* 2016;**30**:311–3.

71. Minagawa A. Dermoscopy-pathology relationship in seborrheic keratosis. *J*

Dermatol 2017;**44**:518–24.

72. Álvarez-Salafranca M, Ara M, Zaballos P. Dermoscopy in Basal Cell Carcinoma: An Updated Review. *Actas Dermosifiliogr (Engl Ed)* 2021;**112**:330–8.

73. Braun RP, Rabinovitz HS, Oliviero M, Kopf AW, Saurat J-H. Dermoscopy of pigmented skin lesions. *J Am Acad Dermatol* 2005;**52**:109–21.

74. Bono A, Maurichi A, Moglia D, *et al.* Clinical and dermatoscopic diagnosis of early amelanotic melanoma. *Melanoma Res* 2001;**11**:491–4.

75. Bories N, Dalle S, Debarbieux S, Balme B, Ronger-Savlé S, Thomas L. Dermoscopy of fully regressive cutaneous melanoma. *Br J Dermatol* 2008;**158**:1224–9.

76. Guitera P, Menzies SW, Longo C, Cesinaro AM, Scolyer RA, Pellacani G. In vivo confocal microscopy for diagnosis of melanoma and basal cell carcinoma using a two-step method: analysis of 710 consecutive clinically equivocal cases. *J Invest Dermatol* 2012;**132**:2386–94.

77. Papageorgiou V, Apalla Z, Sotiriou E, *et al.* The limitations of dermoscopy: false-positive and false-negative tumours. *J Eur Acad Dermatol Venereol* 2018;**32**:879–88.

78. Pizzichetta MA, Polesel J, Perrot JL, *et al.* Amelanotic/hypomelanotic lentigo maligna: Dermoscopic and confocal features predicting diagnosis. *J Eur Acad Dermatol Venereol* 2023;**37**:303–10.

79. Russo T, Pampena R, Piccolo V, *et al.* The prevalent dermoscopic criterion to distinguish between benign and suspicious pink tumours. *J Eur Acad Dermatol Venereol* 2019;**33**:1886–91.

80. Pellacani G, Farnetani F, Ciardo S, *et al.* Effect of Reflectance Confocal Microscopy for Suspect Lesions on Diagnostic Accuracy in Melanoma: A Randomized Clinical Trial. *JAMA Dermatol* 2022;**158**:754–61.

81. Cinotti E, Labeille B, Debarbieux S, *et al.* Dermoscopy vs. reflectance confocal microscopy for the diagnosis of lentigo maligna. *J Eur Acad Dermatol Venereol* 2018;**32**:1284–91.

CHAPTER 7

7. TABLES AND FIGURES

7.1 Tables

Table 1 - Dermoscopic and RCM criteria

Dermoscopy criteria	Definitions
Vascular criteria	
Dotted vessels	Red-colored dots that are usually arranged fairly closely
Comma vessels	Curved vessels that appear to take the shape of a comma. These vessels tend to appear slightly out of focus, as their deeper location within the dermis does not allow for sharp visualization under dermoscopy.
Linear irregular vessels	Linear vessels, which are usually irregular in width and shape
Glomerular vessels	Tortuous vessels, frequently arranged in clusters and resembling the glomerular apparatus of the kidney
Hairpin vessels	Vascular loops resembling a hairpin, which may be twisted in morphology; typically surrounded by a whitish halo when occurring in keratinizing tumors
Arborizing vessels	Vessels that resemble tree branches in morphology, bright red in color and sharply focused; sometimes larger vessels branch irregularly into finer capillaries
Fine teleangiectasia	Fine, red, focused, linear, and barely branching vessels
Reddish pseudonetwork	Erythema located between keratotic (and targetoid) hair follicles, that forms a peculiar strawberry- like pattern
Polymorphous vessels	A combination of 2 or more different types of vascular structures
Pink-red homogeneous colour	Pink-red structureless background
Pigmentation criteria	
Peppering	Speckled multiple blue-gray granules within a hypopigmented area
Black-brown dots/globules	Symmetrical, round to oval, well-demarcated structures that may be brown or black
Blue-gray globules	Symmetrical, round to oval, well-demarcated structures usually large than 0.1 cm that may be blue or gray.
Leaf-like structures	Bulbous extensions connected to a common base
Spoke-wheel/Concentric structures	Radial projections connected to a more strongly pigmented central axis; these projections are occasionally poorly defined and appear as globular structures with a darker center
Peripheral pigment network	A grid-like network consisting of pigmented lines and hypopigmented holes ath the periphery of the lesions, usually fading centrifugally.

Atypical network	Nonuniform network with darker and/or broadened lines and “holes” that are heterogeneous in area and shape, the lines are often hyperpigmented and may end abruptly at the periphery
Negative pigment network	A grid-like network consisting of hypopigmented lines and pigmented holes
Streaks/Pseudopods	Linear extensions or fingerlike projections at the periphery of a lesion
Remnants of pigmentation	Discrete pigment with no discernible structures, at the periphery or diffuse within the lesion; sometimes peppering is detectable nearby
Pigmented structureless area	Wide area devoid of any discernible structures (eg, globules, network)
Other criteria	
Surface scales	White structureless area at the surface of a lesion, usually easily datachable
Erosions	Reddish-brown or yellow-orange areas, smaller than those associated with ulceration
Ulceration	Orange-red structureless areas often with serosanguineous discharge.
White/Wide follicular openings	Yellowish keratotic plugs within the hair follicles, resulting in a whitish-yellowish ‘targetoid-like’ appearance
Milia-like cysts/Comedo-like openings	Milia-like cysts are round whitish or yellowish structures that are seen commonly, but not exclusively, in seborrheic keratosis under non-polarized dermoscopy/Dark roundish structures, and clinically, can be appreciated as surface invaginations.
Central scar-like area	Central white patch often well demarcated with an irregular outline that sometimes appears stellate.
White streaks	Orthogonal or parallel white lines that can only be visualized by polarized dermoscopy
Rosettes	Four white points, arranged as 4-leaf clover
White-pink background	Pink-white coloration background
Blue-white veil	Irregular, indistinct, confluent blue pigmentation with an overlying white, ground-glass haze
RCM criteria	
Hyperkeratosis	Increased thickness of stratum corneum seen as refractile amorphous material
Regular Honeycombed	Normal pattern of the spinous-granular layers formed by bright polygonal outlines of keratinocytes, about 15–25 mm in diameter, with dark central nuclei
Irregular honeycombed	Abnormal pattern of the spinous-granular layers formed by bright cellular outlines which vary in size and shapes and in the thickness and brightness of the lines.
Disarranged epidermal pattern	Focal or diffuse loss of the normal patterns of the spinous-granular layers (honeycomb or cobblestone) characterized by unevenly distributed bright cells and granular particles
Streaming epidermis	Cells within the tumor islands, or overlying basal or spinous keratinocytes, display nuclei that are elongated and distorted into alignment along the same axis
Round pagetoid cells	Large bright cells with well outlined border and dark nucleus within the epidermis
Dendritic pagetoid cells	Large cells with bright cytoplasm and dark nucleus with clearly visible dendrites connected to the cell

Dark pagetoid cells	Large cells, round to oval in shape, that appear as well-demarcated hyporeflective structures detectable within the honeycombed pattern at the spinosum–granulosum layer, usually distinguished from normal keratinocytes because of their size (at least twice the size of a keratinocyte) and shape (round vs. polygonal).
Tumour island	Round to oval, cord-like or lobulated structures at the level of DEJ or superficial dermis that can be either darker than the surrounding epidermis or dermis (“dark silhouettes”) or bright well-demarcated structures.
Clefting	Dark slit-like space observed between tumor island and surrounding dermis
Wide interpapillary area	Space between dermal papillae wider than normal surrounding skin
Dense nest	Compact aggregates with sharp margin and similar cells in morphology and refractivity
Dense and sparse nest	Nondiscrete aggregates with margins that may be sharp or undefined; usually cells are not tightly aggregated within the nest
Polycyclic papillae	Increase in the density of the dermal papillae that presents as bright contours in a polycyclic shape
Melanophages	Plump, bright stellate cells with fuzzy borders, found in the upper dermis
Thickened collagen bundles	Fibrous tracts within the dermis
Atypical junctional cells	Large cells showing a bright cytoplasm with clearly outlined borders and sharply contrasted dark nucleus inside, roundish to oval in shapes, sometimes presenting dendritic-like structures, located at the dermal–epidermal junction
Edged ring pattern	Dermal papillae demarcated by a rim of bright cells (pigmented basal keratinocytes and melano- cytes). The appearance is that of bright rings
Non-edged ring pattern	Dermal papillae without a demarcating bright rim at the DEJ, but separated by a series of large reflecting cells
Meshwork pattern	Distinctive mesh characterized by small dark holes surrounded by clearly thickened inter-papillary spaces
Clod pattern	Numerous densely packed clods, constituted by clusters of melanocytes usually within dermal papillae

Table 2 – Patient demographics and lesion location

	Total No.=184, 100%	non-fAHM No.=137, 74.5%	fAHM No.=47, 25.5%	P value
Female, No *(%)*	87 (47.3)	68 (49.6)	19 (40.4)	.275
Age at diagnosis, *mean yrs ±SD (range)*	57.6 ±14.2 (19-95)	55.8 ±13.8 (19-95)	62.6 ±14.2 (28-84)	**.004**
Anatomical location				
Head and neck	19 (10.3)	15 (10.9)	4 (8.5)	**.007**
Trunk	110 (59.8)	84 (61.3)	26 (55.3)	
Upper limb	28 (15.2)	14 (10.2)	14 (29.8)	
Lower limb	27 (14.7)	24 (17.5)	3 (6.4)	

Abbreviations: SD, standard deviation; *fAHM*, flat amelanotic-hypomelanotic melanoma; *non-fAHM,* non-flat amelanotic-hypomelanotic melanoma.

Table 3 – Dermoscopy and combined dermoscopy/RCM assessment compared to histopathologic diagnoses

	Dermoscopy evaluations						**Dermoscopy + RCM evaluations**					
	Evaluator A			Evaluator B			Evaluator A			Evaluator B		
	Total	non-fAHM	fAHM	Total	non-fAHM	fAHM	Total	non-fAHM	fAHM	Total	non-fAHM	fAHM
	No.=184	No.=137 (74.5%)	No.=47 (25.5%)	No.=184	No.=137 (74.5%)	No.=47 (25.5%)	No.=184	No.=137 (74.5%)	No.=47 (25.5%)	No.=184	No.=137 (74.5%)	No.=47 (25.5%)
fAHM	51 (27.7)	15 (10.9)	36 (76.6)	69 (37.5)	28 (20.4)	41 (87.2)	66 (35.9)	27 (19.7)	39 (82.9)	70 (38.0)	27 (19.7)	43 (91.5)
Non-fAHM												
BCC (No.=62)	84 (45.6)	74 (54.0)	10 (21.3)	71 (38.6)	66 (48.2)	5 (10.6)	70 (38.0)	63 (45.9)	7 (14.9)	64 (34.8)	60 (43.8)	4 (8.5)
DF (No.=22)	21 (11.4)	20 (14.6)	1 (2.1)	17 (9.2)	17 (12.4)	0 (0.0)	20 (10.9)	19 (13.9)	1 (2.1)	21 (11.4)	21 (15.3)	0 (0.0)
LPLK (No.=7)	3 (1.6)	3 (2.2)	0 (0.0)	3 (1.6)	3 (2.2)	0 (0.0)	4 (2.2)	4 (2.9)	0 (0.0)	5 (2.7)	5 (3.6)	0 (0.0)
AK (No.=5)	4 (2.2)	4 (2.9)	0 (0.0)	3 (1.6)	3 (2.2)	0 (0.0)	1 (0.5)	1 (0.7)	0 (0.0)	4 (2.2)	4 (2.9)	0 (0.0)
BD (No.=5)	4 (2.2)	4 (2.9)	0 (0.0)	4 (2.2)	4 (2.9)	0 (0.0)	2 (1.1)	2 (1.5)	0 (0.0)	2 (1.1)	2 (1.5)	0 (0.0)
SK (No.=5)	1 (0.5)	1 (0.7)	0 (0.0)	4 (2.2)	4 (2.9)	0 (0.0)	3 (1.6)	3 (2.2)	0 (0.0)	2 (1.1)	2 (1.5)	0 (0.0)
Melanocytic nevus (No.=31)	16 (8.7)	16 (11.7)	0 (0.0)	13(7.1)	12 (8.8)	1 (2.1)	18 (9.8)	18 (13.1)	0 (0.0)	15 (8.1)	15 (10.9)	0 (0.0)

Abbreviations: fAHM, flat amelanotic-hypomelanotic melanoma; *non-fAHM,* non-flat amelanotic-hypomelanotic melanoma; BCC, basal cell carcinomas; DF, dermatofibroma; LPLK, lichen planus-like keratosis; AK, actinic keratosis; BD, Bowen diseases; SK, seborrheic keratosis.

Table 4 - Sensitivity and specificity for dermoscopy and combined dermoscopy and RCM evaluations

	Sensitivity, *% (95% CI)*	Specificity *% (95% CI)*	AUC
Dermoscopy evaluations			
Evaluator A	76.6 (62.0-87.7)	89.0 (82.6-93.7)	0.82
Evaluator B	85.1 (71.7-93.8)	79.5 (71.8-86.0)	0.82
Dermoscopy + RCM evaluations			
Evaluator A	83.0 (69.2-92.4)	80.3 (72.6-86.6)	0.81
Evaluator B	91.5 (79.6-97.6)	80.3 (72.6-86.6)	0.86

Abbreviations: CI, confidence interval; AUC, area under the curve; RCM, reflectance confocal microscopy

Table 5 - Univariate and multivariate models for diagnosis (fAHM vs non-fAHM)

	Univariate			Multivariate		
	OR	95%CI	P value	OR	95%CI	P value
Demographic and clinical criteria						
Age at diagnosis, *mean yrs ±SD(range)*	1.03	1.01-1.06	**.005**			
Dermoscopy criteria						
Vessels:						
Dotted	4.22	1.94-9.16	**<.001**			
Linear irregular	6.05	2.93-12.45	**<.001**	4.26	1.51-12.01	**.006**
Arborizing	0.23	0.09-0.56	**.001**			
Fine teleangiectasia	0.10	0.01-0.82	**.03**			
Polymorphous vessels	5.92	2.61-13.44	**<.001**			
Peripheral pigment network	2.52	1.22-5.21	**.01**	6.07	1.83-20.15	**.003**
Negative pigment network	7.13	2.29-22.17	**.001**			
Remnants of pigmentation	4.92	2.14-11.30	**<.001**	4.30	1.27-14.55	**.01**
White-pink background	0.16	0.05-0.47	**.001**			
RCM criteria						
Epidermal pattern:						
Irregular honeycomb	13.6	3.11-59.5	**.001**	9.98	1.91-51.96	**.006**
Disarranged	44.4	8.92-220.6	**<.001**	15.22	2.18-106.23	**.006**
Streaming epidermis	0.16	0.05-0.49	**.001**			
Round pagetoid cells	12.18	5.55-26.73	**<.001**			
Dendritic pagetoid cells	8.69	4.13-18.28	**<.001**	3.77	1.25-11.26	**.01**
Hyporeflective pagetoid cells	16.07	1.82-141.43	**.01**	27.05	1.57-465.50	**.02**
Tumour island	0.20	0.08-0.49	**<.001**			
Clefting	0.20	0.07-0.55	**.002**			
Dense and sparse nest	10.32	4.82-22.09	**<.001**	3.68	1.24-10.96	**.01**
Sheet of cells	3.78	1.28-11.08	**.015**			
Thickened collagen bundles	0.17	0.06-0.43	**<.001**			
Atypical junctional cells	10.65	4.95-22.90	**<.001**			

Abbreviations: OR, odds ratio*; SD,* standard deviation; CI, confidence interval; *fAHM*, flat amelanotic-hypomelanotic melanoma; *non-fAHM,* non-flat amelanotic-hypomelanotic melanoma

Table 6 - fAHM Index: worksheet to assist in personalized score calculation.

	Score	Personalized Score
Dermoscopy features		
Linear irregular vessels	4.5	
Peripheral pigmented network	5.5	
Remnants of pigmentation	4.5	
RCM features		
Irregular honeycomb pattern	7.0	
Disarranged epidermal pattern	8.5	
Dendritic pagetoid cells	4.0	
Hyporeflective pagetoid cells	10	
Dense and sparse nests	4.0	
	Total score	

Figure 1- Flowchart showing inclusion and exclusion criteria

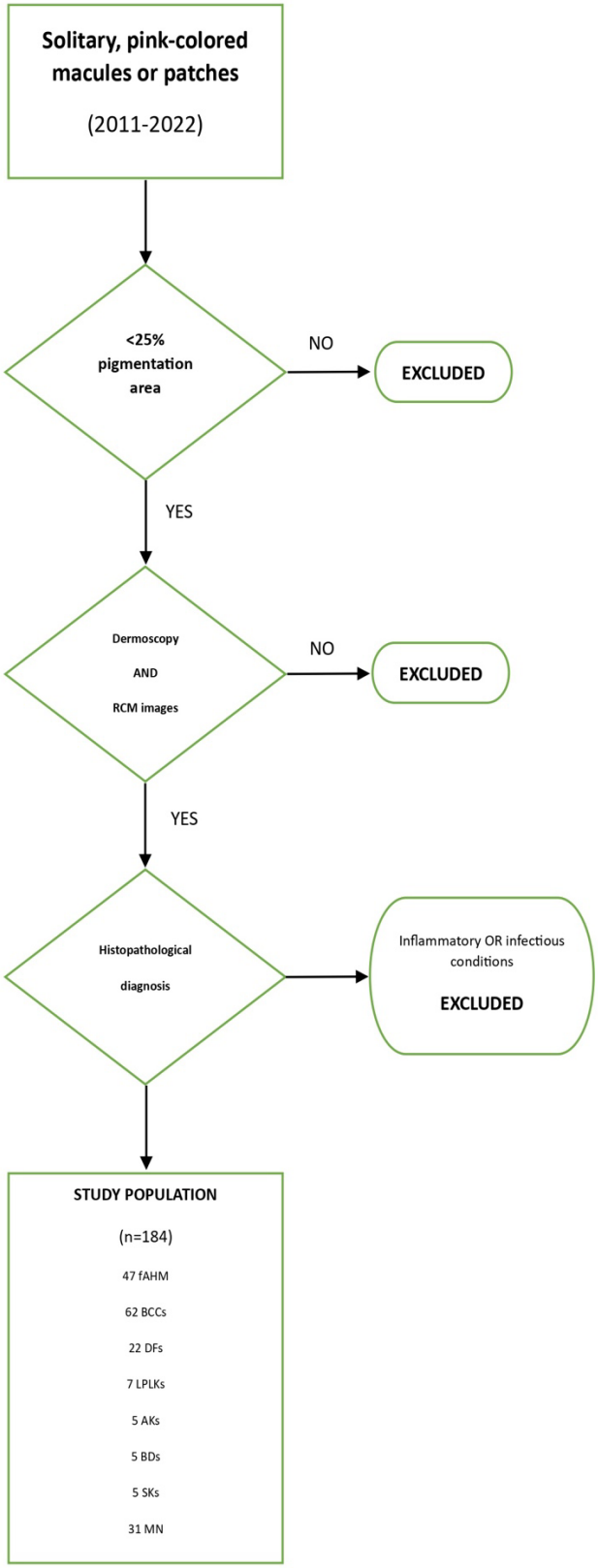

Figure 2 – Nomogram analysis and diagnostic accuracy of the nomogram

(a) Nomogram analysis showing single independent features in dermoscopy and RCM associated with fAHM diagnosis and relative scores; the total score is matched on the probability line; (b) diagnostic accuracy of the nomogram.

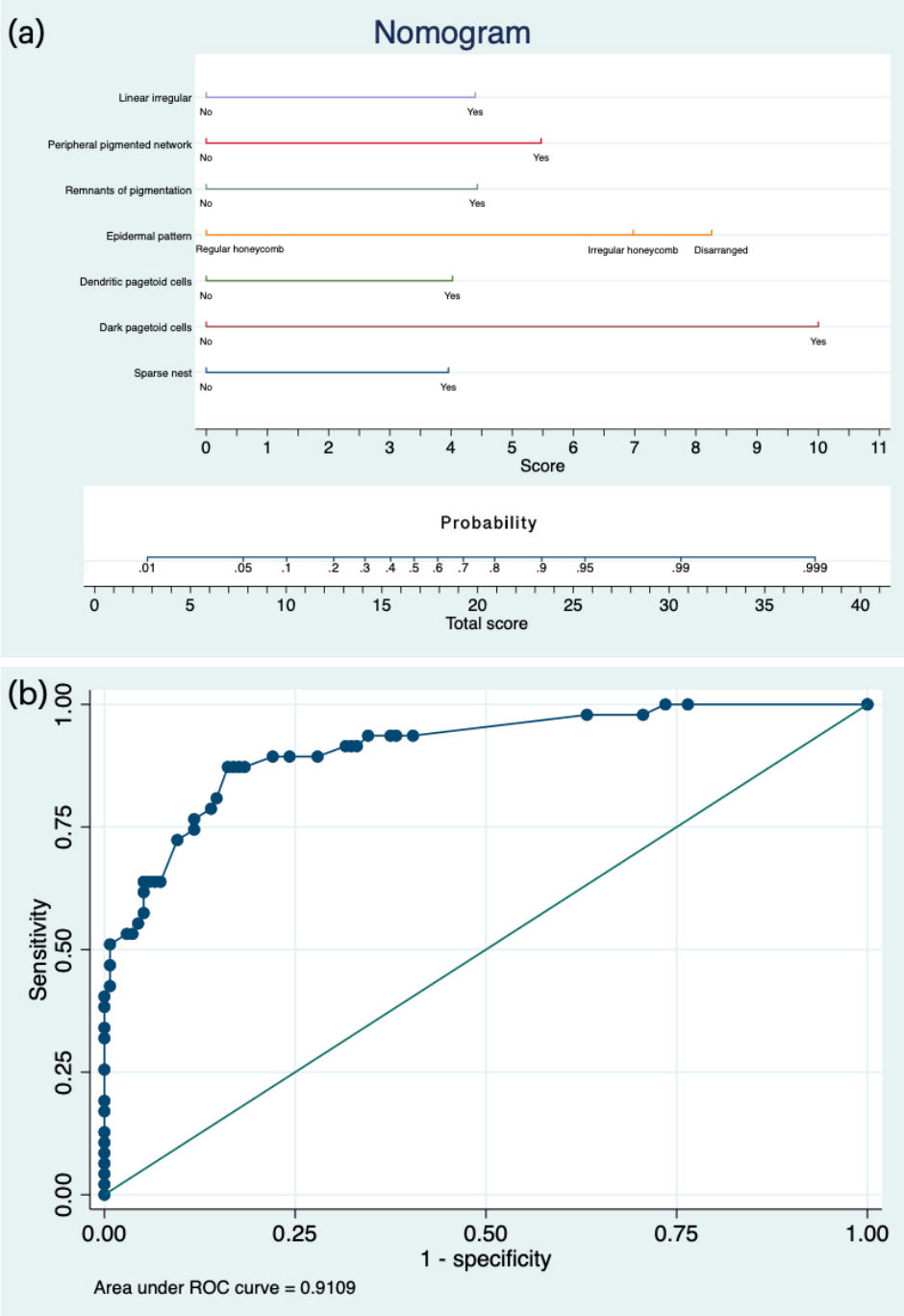

Figure 3 - fAHM Index applied to selected solitary flat pink lesions

(a) Clinical image (inset) shows a pink macule on the trunk of a 64-year-old woman. Dermoscopy shows a pinkish hue with a peripheral partially interrupted light-pigmented network (green arrow), remnants of pigmentation (black arrow), and linear irregular vessels (blue arrow). (b) RCM at the spinous-granular layer shows a disarranged epidermal pattern (yellow asterisk), and hyporeflective pagetoid cells (pink arrows). fAHM Index=33/38 (probability 0.99-0.999) Histhopathologic diagnosis: Amelanotic melanoma (Breslow thickness 0.6 mm).

(c) Clinical image (inset) shows a pink macule on the trunk of an 80-year-old man. Dermoscopy shows a pink hue with linear irregular vessels (blue arrows). No other melanoma diagnostic criteria are detectable at dermoscopy (d) RCM at the spinous-granular layer shows a disarranged epidermal pattern (yellow asterisk), hyporeflective pagetoid cells (pink arrows), and dendritic pagetoid cells (red arrow). fAHM Index=27/38 (probability 0.95-0.99) Histhopatologic diagnosis: Amelanotic melanoma (Breslow thickness 0.5 mm).

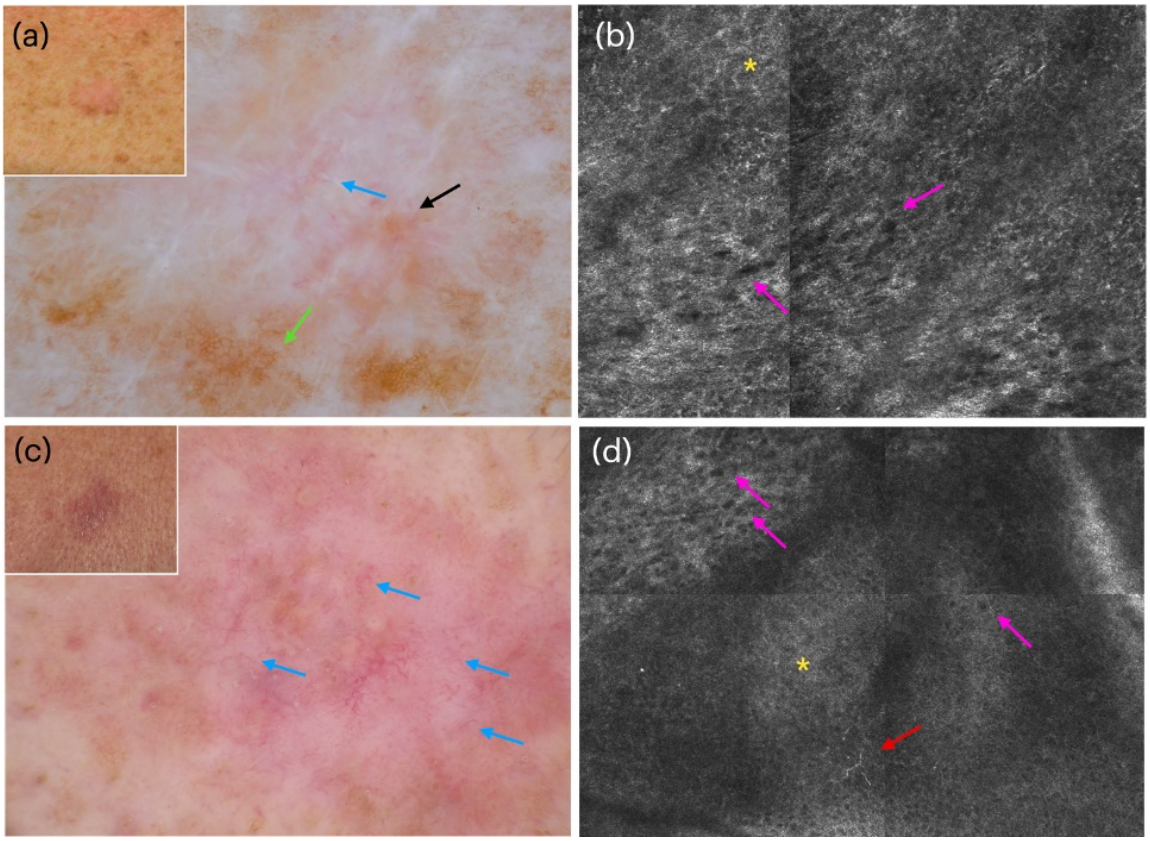
(a)
(b)
(c)
(d)

APPENDIX

LIST OF SCIENTIFIC PUBLICATIONS DURING MY PhD COURSE

1. Ambrosio L., Pogorzelska-Antkowiak A., Retrosi C., Di Lella G., **Spadafora M**., Zalaudek I., Longo C., Pellacani G., Conforti C. Reflectance Confocal Microscopy and Dermoscopy for the Diagnosis of Solitary Hypopigmented Pink Lesions: A Narrative Review (2024) Cancers, 16 (17), art. no. 2972 DOI: 10.3390/cancers16172972
2. Longo C., Lippolis N., Lai M., **Spadafora M**., Kaleci S., Condorelli A.G., Lombardi M., Pampena R., Argenziano G., Nazzaro G., Scalvenzi M., Akay B.N., Broganelli P., Fargnoli M.C., Paoli J., Yélamos O., Pellacani G., Borsari S., Lallas A Dermoscopic features of trichoepithelioma: A multicentre observational case–control study conducted by the International Dermoscopy Society (2023) Journal of the European Academy of Dermatology and Venereology, 37 (10), pp. e1253 - e1255 DOI: 10.1111/jdv.19262
3. Guida S., Longo C., Amato S., Rossi A.M., Manfredini M., Ciardo S., **Spadafora M**., Nisticò S.P., Mercuri S.R., Rongioletti F., Zerbinati N., Pellacani G Laser Treatment Monitoring with Reflectance Confocal Microscopy (2023) Medicina (Lithuania), 59 (6), art. no. 1039 DOI: 10.3390/medicina59061039

4. Paganelli A., Zaffonato M., Donati B., Torricelli F., Manicardi V., Lai M., **Spadafora M**., Piana S., Ciarrocchi A., Longo C. Molecular and Histopathological Characterization of Metastatic Cutaneous Squamous Cell Carcinomas: A Case–Control Study (2024) Cancers, 16 (12), art. no. 2233 DOI: 10.3390/cancers16122233
5. Paganelli A., **Spadafora M**., Navarrete-Dechent C., Guida S., Pellacani G., Longo C. Natural language processing in dermatology: A systematic literature review and state of the art (2024) Journal of the European Academy of Dermatology and Venereology DOI: 10.1111/jdv.20286
6. **Spadafora M**., Megna A., Lippolis N., Cavicchi M., Borsari S., Piana S., Guida S., Kaleci S., Chester J., Pellacani G., Longo C. Dermoscopy and reflectance confocal microscopy of solitary flat pink lesions: A new combined score to diagnose amelanotic melanoma (2024) Journal of the European Academy of Dermatology and Venereology DOI: 10.1111/jdv.19991
7. **Spadafora M**., Santandrea G., Lai M., Borsari S., Kaleci S., Banzi C., Mandato V.D., Pellacani G., Piana S., Longo C.Clinical Review of Mucosal Melanoma: The 11-Year Experience of a Referral Center (2023) Dermatology Practical and Conceptual, 13 (1), art. no. e2023057 DOI: 10.5826/dpc.1301a57
8. Longo C., Guida S., Mirra M., Pampena R., Ciardo S., Bassoli S., Casari A., Rongioletti F., **Spadafora M**., Chester J., Kaleci S., Lai M., Magi S., Mazzoni L., Farnetani F., Stanganelli I., Pellacani G Dermatoscopy and reflectance confocal microscopy for basal cell carcinoma diagnosis and diagnosis

prediction score: A prospective and multicenter study on 1005 lesions (2024) Journal of the American Academy of Dermatology, 90 (5), pp. 994 - 1001 DOI: 10.1016/j.jaad.2024.01.035

9. **Spadafora M**, Farnetani F, Borsari S, Kaleci S, Porat D, Ciardo S, Stanganelli I, Longo C, Pellacani G, Scope A. Clinical, dermoscopic and reflectance confocal microscopy characteristics of negative pigment network among Spitzoid neoplasms. Journal of Investigative Dermatology (under review)
10. **M Spadafora**, R Pampena, K. Peris, L. Del Regno, L. Cornacchia, M.C Fargnoli, C. Pellegrini, P. Quaglino, S. Ribero, P.G. Calzavara-Pinton, MC Arisi, M. Mirra, M.Raucci, S Kaleci, J Chester, G Pellacani, C Longo. Efficacy comparison of passive versus active educational interventions in non-medical individuals for atypical skin melanocytic lesion identification. Journal of European Academy of Dermatology (under review)
11. **Spadafora M**, Morsia S, Di Lernia VG, Pellacani G, Longo C Off-Label Use of Topical Ruxolitinib in Dermatology: A Systematic Literature Review and Current Perspectives Journal of European Academy of Dermatology (under review)